Eur. Phys. J. B **52**, 107–111 (2006)
DOI: 10.1140/epjb/e2006-00274-x

THE EUROPEAN PHYSICAL JOURNAL B

Fractal formations in the Lattice Limit Cycle model

G.A. Tsekouras[1,2] and A. Provata[1,a]

[1] Institute of Physical Chemistry, National Center for Scientific Research "Demokritos", 15310 Athens, Greece
[2] Department of Physics, University of Athens, 10679 Athens, Greece

Received 14 October 2005
Published online 6 July 2006 –

Abstract. We examine the fractal patterns arising in the Lattice Limit Cycle model, when it is restricted on square and fractal lattices. We show that, for processes taking place on regular 2d substrates, the fractal dimensions depend on the kinetic constants and we have observed a sharp phase-transition from uniform 2d spatial distributions ($d_f = 2$) when the kinetic parameters are near the Hopf bifurcation point, to a $d_f \neq 2$ inside the limit cycle region. For processes taking place on substrates which contain inactive sites, we observe nucleation of homologous species around inactive regions leading to poisoning, when the active sites are distributed in a fractal manner on the substrate. This is less frequent in cases where the active sites are distributed uniformly and randomly on the lattice leading, normally, to non-trivial steady states.

PACS. 05.45.-a Nonlinear dynamics and chaos – 05.45.Df Fractals – 05.65.+b Self-organized systems

1 Introduction

Previous research in heterogeneous catalysis [1–6] and in population biology [7,8] demonstrates complex spatiotemporal pattern formation and nonlinear front propagation in a wide variety of systems. This kind of spatiotemporal complexity arises in multiple time and/or space scales. It is thus necessary to understand, using minimal models, the generic, and possibly universal, underlying mechanisms that lead to the production of complexity in low dimensional systems.

In this spirit it has been recently shown that complex non-linear spatiotemporal behaviour and fractality appear spontaneously in the Lattice Lotka-Volterra (LLV) model [9,10]. This model involves predator-prey type of interactions and when implemented on lattice via the Kinetic Monte-Carlo (KMC) method the various species segregate in clusters with fractal boundaries [10]. At the mean field level the LLV model is conservative. An alternative, more stable, interacting particle model was later introduced, the Lattice Limit Cycle (LLC) model [11]. The LLC model was constructed to possess dissipative dynamics, since conservative dynamics is unstable under the influence of external forces or noise. This model at the MF level exhibits a limit cycle behaviour and is thus more robust under the influence of noise. The LLC model, which involves a 4th order non-linearity, has been shown to produce a variety of dynamical patterns with fractal structure [16].

In the current study we concentrate on the quantitative description of the fractal patterns observed in LLC as a function of the kinetic parameters. In particular, we study how the fractal dimensions change as we pass through the Hopf bifurcation point and into the limit cycle region. We show that there is an abrupt transition of the fractal dimension as we go through the bifurcation point, while the fractal dimension remains almost constant throughout the limit cycle region of the parametric space.

2 The Lattice Limit Cycle model

The LLC model is summarized by the following reaction scheme [11]:

$$2X_1 + 2X_2 \xrightarrow{k_1} 3X_2 + S \tag{1a}$$

$$X_1 + S \xrightarrow{k_2} 2X_1 \tag{1b}$$

$$X_2 + S \xrightarrow{k_3} 2S. \tag{1c}$$

Here X_1 and X_2 are the two reactive species and S denotes the empty lattice sites. Step (1a) describes a quadrimolecular autocatalytic reaction between the two species X_1 and X_2, step (1b) a cooperative adsorption of X_1 while step (1c) a cooperative desorption of X_2. The autocatalytic nature of these reactions is the driving force behind the nonlinear spatiotemporal phenomena that we study in the sequel. In the predator-prey frame, X_1 represents the prey, X_2 the predator while S is the empty space. In that sense, equation (1a) represents the non-linear predator-prey interactions, equation (1b) the birth of new prey while equation (1c) the death of the predators.

[a] e-mail: aprovata@limnos.chem.demokritos.gr

2.1 Kinetic mean field equations

The rate equations that arise from reactive scheme (1), after using the naturally arising conservation condition $x_1 + x_2 + s = 1$, are [11]:

$$\frac{dx_1}{dt} = -2k_1 x_1^2 x_2^2 + k_2 x_1(1 - x_1 - x_2) \tag{2a}$$

$$\frac{dx_2}{dt} = k_1 x_1^2 x_2^2 - k_3 x_2(1 - x_1 - x_2). \tag{2b}$$

In equation (2) x_1, x_2 and s stand for the global concentrations of X_1, X_2 and empty sites respectively. The above system has four steady state solutions, namely

$$P_1 = (0, 0) \tag{3a}$$

$$P_2 = (1, 0) \tag{3b}$$

$$P_3 = (0, 1) \tag{3c}$$

$$P_4 = \left(\sqrt[3]{[1+K]\, k_3^2/k_1 k_2} + \sqrt[3]{[1-K]\, k_3^2/k_1 k_2}, \right.$$
$$\left. \sqrt[3]{[1+K]\, k_2^2/8k_1 k_3} + \sqrt[3]{[1-K]\, k_2^2/8k_1 k_3} \right) \tag{3d}$$

where

$$K = \sqrt{1 + (2k_3 + k_2)^3/27 k_1 k_2 k_3}. \tag{4}$$

The first three are saddle points,while the fixed point P_4 is of non-trivial stability. Depending on the parameters, P_4 can pass from stable node to stable focus and to unstable focus. During the transition from a stable focus to an unstable focus (Hopf bifurcation) a limit cycle is generated.

2.2 Kinetic Monte Carlo method

On lattice simulations have been used since the pioneering work of Ziff, Gulari and Barshad [12] to understand the influence of the substrate structure and of the local fluctuations on the dynamics and the steady state properties of interacting particle systems [13–15].

To simulate the on-lattice LLC dynamics we use the KMC algorithm introduced in reference [11] and is summarized in the following steps:

- set the initial state of each lattice site among the three possible states (X_1, X_2 or S);
- at each Elementary Time Step (ETS), select one random site;
- if the selected site is X_1 and there are two neighboring X_2 and one X_1 then with probability p_1 proportional to k_1 perform reaction (1a);
- similarly we work for the other two reactive steps; and
- a Monte Carlo Time Step (MCS) is the time needed to visit each site once on average (for a square lattice 1 MCS = L^2 ETS).

It has already been pointed out that when the LLC is realized on a two-dimensional lattice spontaneous nucleation processes take place [16]. During these processes, clusters of homologous species are built up. These clusters play the role of interacting local oscillators and for each of them the MF theory works quite adequately but since they are out of phase, the global concentrations do not demonstrate oscillations and are not thus correctly described by the MF equations.

When observing closely the dynamical structures of the LLC, self-similar characteristics can be associated with the shorter length scales. In Figure 1 we present some typical snapshots for the spatiotemporal evolution of the system. Starting from a uniform random state which contains the same percentage of X_1, X_2 and S particles, the dynamics drive the system to segregate and form dynamical islands which compete with one-another through their boundaries. The motion of the boundaries can be characterised as "color diffusion", since in this model the particles are not allowed to move from one site to another (no normal diffusion) but they change their nature (color) through interaction.

3 Fractal dimensions

To quantify the self-similar properties of the spatiotemporal formations we calculate the fractal dimension d_f using the typical box-counting method [17,18]. We partition the $L \times L$ lattice into boxes of size $\ell \times \ell$ and count the number $N(\ell)$ of boxes that contain part of the fractal. The function $N(\ell)$ takes the form $N(\ell) \sim \ell^{-d_f}$. We can thus calculate the box-counting fractal dimension d_f as the slope of the function $N(\ell)$ vs. ℓ in a double logarithmic graph.

Performing a fractal analysis for a lattice governed by LLC dynamics we obtain graphs such as the one depicted in Figure 2. In this figure the system size is $L^2 = 1000 \times 1000$ sites and the run time is $t = 10\,000$ MCS. (The steady state is established after about 1000 MCS.) The kinetic parameters are $k_1 = 120$, $k_2 = 0.5$ and $k_3 = 0.8$. Each data set (and corresponding species) demonstrates a well defined scale ℓ_{cut} above which the value of the fractal dimension d_f becomes equal to 2, while below this length the structures are fractal with $d_f < 2$. The different species may in general present different values of ℓ_{cut}. The meaning of this is that there is an upper cut-off scale below which the formations present fractality while above it the formations are uniformly distributed on the square lattice and they homogeneously cover the entire two-dimensional space, hence $d_f = 2$. In addition, the data demonstrates a cut-off in the low length scales due to finite size effects. For the present parameter values the lower cut-off takes place at $l = 4$; it is not shown in Figure 2 (the x-axis starts from $l = 4$) but is taken into account when computing d_f.

In our simulations we have run systems of size $L^2 = 1000 \times 1000$ sites, for times up to 60 000 MCS, for different parametric values (with k_1 ranging from 8 to 300 and $k_2 = 0.5$ and $k_3 = 0.8$). The lower values of k_1 correspond to points that are located close to the Hopf bifurcation

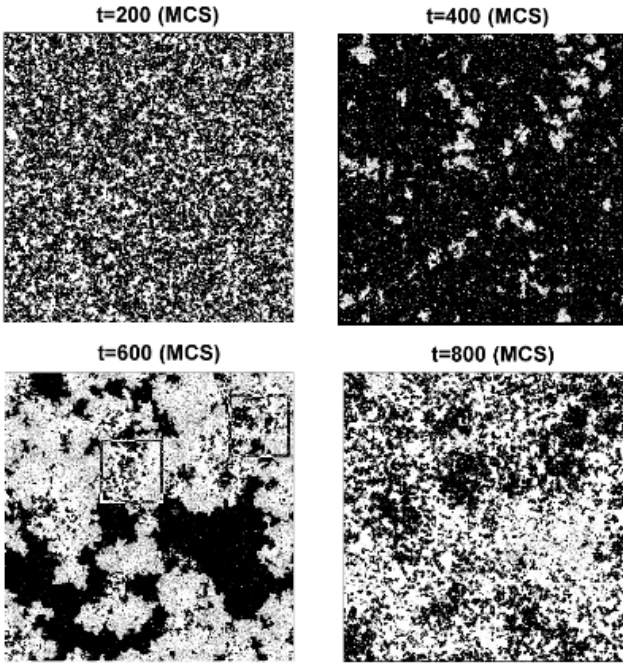

(a)

(b)

Fig. 1. (a) Typical snapshots of the evolution of the system for $k_1 = 50$, $k_2 = 0.5$ and $k_3 = 0.8$. The black sites represent X_1, the gray X_2 while the white represent S, and (b) Blowups of the marked regions for $t = 600$ MCS.

and thus for these values oscillations are less robust and lattice poisoning can be observed. For larger values of k_1 the system is located deep into the limit cycle parametric region, producing oscillations and strong manifestation of the fractal spatiotemporal patterns. We have measured the turnover point and the fractal dimension for all three

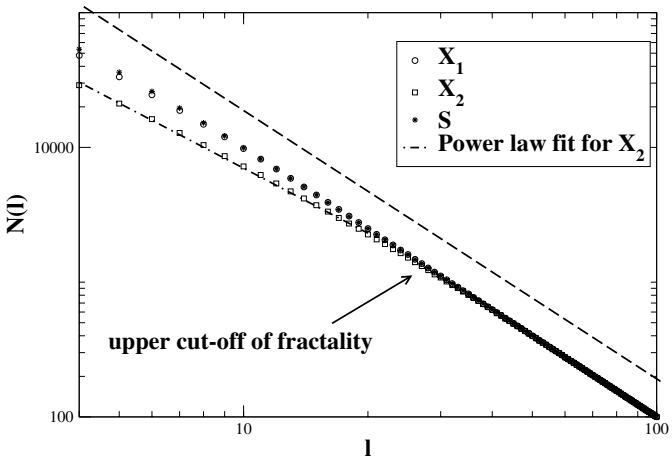

Fig. 2. Double logarithmic plot of the number of boxes $N(\ell)$ containing part of the fractal as a function of the box size ℓ. The slope of the dashed line is -2. The "upper cut-off of fractality" for species X_2 is depicted. The fractal analysis is done for $t = 10\,000$ MCS in a simulation with $k_1 = 120$, $k_2 = 0.5$ and $k_3 = 0.8$. The lattice size is $L^2 = 1000 \times 1000$ sites.

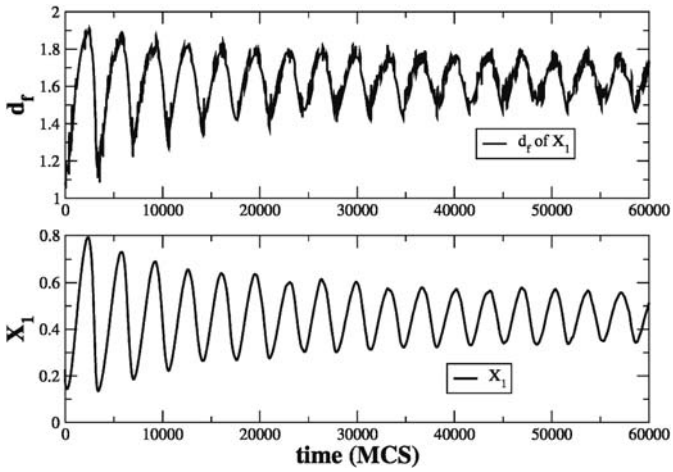

Fig. 3. In the upper graph the fractal dimension d_f for species X_1 is presented as a function of time while on the lower graph the concentration X_1 also as a function of time is drawn for comparison. The kinetic parameters are $k_1 = 300$, $k_2 = 0.5$ and $k_3 = 0.8$ and are located inside the limit cycle region.

species every 1 MCS throughout the simulation and we have calculated the mean value of the fractal dimension.

In Figure 3 we present a typical temporal evolution of d_f for species X_1 and on the same graph we plot the average concentration of X_1 calculated over the entire lattice. The calculation of d_f via the box counting method is also performed on the entire lattice. It can be readily observed that there is a positive correlation between the concentration of X_1 and the fractal dimension since the two graphs present the same oscillatory behaviour and their oscillations are also in phase. At the initial stages of evolution, when the concentration of X_1 tends to cover the system almost completely (eg. $x_1 > 0.7$), the fractal dimension tends to the value 2, which is expected for

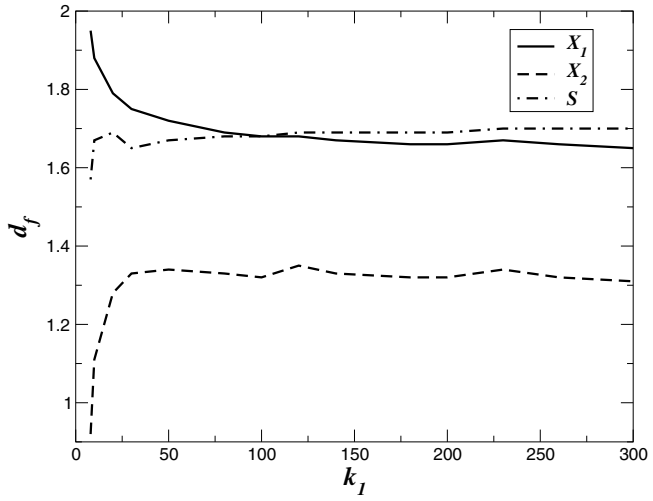

Fig. 4. The box-counting fractal dimension d_f for the three species as a function of k_1. The other kinetic constants are $k_2 = 0.5$ and $k_3 = 0.8$. The fractal dimension is averaged over runs of 60 000 MCS.

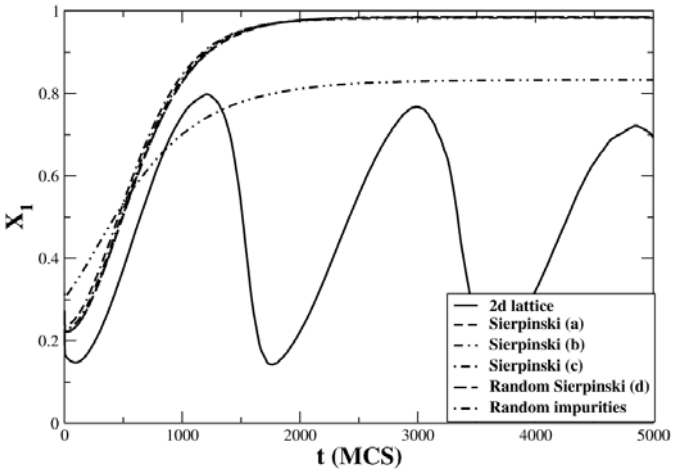

Fig. 5. Concentration X_1 as a function of time for a normal 2d lattice, four different Sierpinski carpets and a lattice with random impurities. The kinetic parameters are $k_1 = 150$, $k_2 = 0.5$ and $k_3 = 0.8$.

a lattice completely covered by X_1. As the system approaches the steady state the amplitudes of x_1 and of the corresponding d_f oscillations decrease approaching a stable value. Still, though oscillations persist for systems of finite size both for x_1 and for the corresponding d_f. As the concentration of X_1 increases tending towards 1, the stochastic noise due to the Monte Carlo processes tends to unify the system and d_f tends to 2. Fractality, in this case, stems from the competitive interactions between domains of different species. The borderline reactions between the different species are governed by the dynamics of equations (2), which have built-in limit cycle oscillations. As was demonstrated in Section 2, the oscillatory behaviour persists locally causing the formation of local oscillators which in turn dictate the competitive domain interactions. Thus the temporal evolution of the domain fractality is drastically influenced by the collective behaviour of these out-of-phase, locally interacting oscillators.

In Figure 4 we present the fractal dimension for X_1, X_2 and S as a function of k_1 for fixed $k_2 = 0.5$ and $k_3 = 0.8$. For these values of k_2 and k_3 the Hopf bifurcation takes place at $k_1 \approx 10$ [11]. We can conclude from this figure that the mean fractal dimension seems to be almost independent of the kinetic parameters when we are inside the limit cycle region. When the Hopf bifurcation is approached (for $k_1 \approx 10$), a poisoned state by X_1 is favored and we have sharp transition where $d_{f(X_1)} \to 2$, $d_{f(X_2)} \to 0$ and $d_{f(S)} \to 0$.

Another aspect worth investigating is the actual value of the upper cut-off of fractality l_{cut} for the three species, introduced earlier in this section. We have found that these values are weakly dependent on the parameters and for X_1 and S it is around 10 while for X_2 it is 35. This large value for the cut-off of X_2 can be attributed to the fact that X_2 is produced through a highly nonlinear reactive step (the quadrimolecular one) and this strong nonlinearity seems to be connected to a more pronounced fractal structure of the corresponding X_2 clusters.

4 Fractal substrates

The importance of the topology of the catalytic surface is well established and has been investigated experimentally using nanostructured catalytic surfaces with spatially modulated reactivity [19]. In a previous study [10], the dynamics of the LLV model was studied when inactive sites are distributed in a fractal manner on the catalytic support. It was shown that the system tends to reach the poisoning states easier and its dynamical behaviour is generally affected. It is thus interesting to conduct the same investigations on the LLC when realized on a fractal lattice.

We have performed simulations using as supports a) a normal two-dimensional lattice with $L = 512$, b) deterministic Sierpinski carpets with $L = 729$ and fractal dimension $D = 1.893$ but different topologies, c) a random Sierpinski carpet with $L = 729$ and fractal dimension $D = 1.893$ and d) a lattice with $L = 729$ but with randomly distributed inactive sites. We set the lattice sizes, dimensionality and inactive to active site ratio in such a way that all lattices considered have the exact same number of active lattice sites. We run a simulation with $k_1 = 150$, $k_2 = 0.5$ and $k_3 = 0.8$. This parametric point is situated well within the limit cycle region. The dynamics take place only on the sites which constitute the fractal (called the active sites), while all other sites are called inactive and in experimental catalysts may be impurities.

In Figure 5 we observe that while in the normal lattice the previously described oscillatory behaviour arises, both for the fractal lattices and for the lattice with random impurities the system goes to "frozen" states. In the case of the fractal lattices, the frozen states are very close to the poisoning by X_2 state, while in the case of random impurities the system freezes in a non-trivial point.

The explanation for this behaviour lies in the fact that, due to nucleation, large clusters of homologous species are created. These clusters cannot react with each other due to

the introduced low topological connectivity and a frozen state arises. The difference between lattices with randomly distributed impurities and the fractal lattices is that the later leads to a state which is very close to poisoning by one species while the former leads to a state where all species coexist.

Another interesting point here is that the exact topological structure of the fractal substrate does not seem to play any role but what appears to be important is the statistics as quantified by the fractal dimension and higher fractal moments. This fact has been previously observed on LLV [10] and could be thus relatively model independent. The investigation of the effects of impurities and/or fractal substrates on reactive dynamics is very interesting since our results suggest that, possibly, by designing the catalytic surfaces with specific topologies we could drive the system to different coexisting states at will.

5 Conclusions

Summarizing, in this work we have studied the pattern formation process in the Lattice Limit Cycle (LLC) model. Fractal structures are observed in the low-length scales (up to a cut-off scale). We have also found that the mean fractal dimension of these patterns seems to be quite insensitive to changes in the kinetic parameters when we stay inside the limit cycle parametric region. When however the Hopf bifurcation is approached the system tends to poisoning and it undergoes a rapid change in the fractal dimension. We have observed that the temporal evolution of the fractal dimension for any species is positively correlated to its concentration evolution over time. We have also examined how the LLC dynamics is modified when the substrate is fractal or includes randomly distributed inactive sites. We have concluded that in both cases the LLC system gravitates away from its 2-d oscillatory behaviour and into frozen states. The fractal substrates however, seem to be more capable to drag the system closer to the poisoning states (in some cases the final concentration of the poisoning species reaches 0.98). It is shown also, that it is the substrate's fractal statistics and not the specific topology of the substrate which dictates the outcome of the process.

Future perspectives of this work would include the investigation of an hierarchy of more complex models, including chaotic ones, in order to derive the model-independent features of these fractal patterns and to understand better the mechanisms through which MF approach fails in that category of models. As mentioned earlier, in this model the particles do not move from one site to another but only change their nature due to the interaction with neighbors. In our future plans the inclusion of particle diffusion will be considered since this process introduces local mixing and may modify the results considerably.

The authors would like to thank Profs. G. Nicolis and F. Baras for helpful discussions. We gratefully acknowledge financial support by the European Union under contract EPEAEK/PYTHAGORAS 70/3/7357.

References

1. R. Imbihl, G. Ertl, Chem. Rev. **95**, 697 (1995)
2. G. Ertl, Science **254**, 1750 (1991)
3. J. Wintterlin, Adv. Catal. **45**, 131 (2000)
4. K.C. Rose, D. Battogtokh, A. Mikhailov, R. Imbihl, W. Engel, A.M. Bradshaw, Phys. Rev. Lett. **76**, 3582 (1996)
5. A. von Oertzen, H.H. Rotermundand, A.S. Mikhailov, G. Ertl, J. Phys. Chem. B **104**, 3155 (2000)
6. C. Voss, N. Kruse, Ultramicroscopy **73**, 211 (1998)
7. J.L. Deneubourg, A. Lioni, C. Detrain, Biol. Bull. **202**, 262 (2002)
8. F. Saffre, J.L. Deneubourg, J. Theor. Biol. **214**, 441 (2002)
9. A. Provata, G. Nicolis, F. Baras, J. Chem. Phys. **110**, 8361 (1999)
10. G.A. Tsekouras, A. Provata, Phys. Rev. E **65**, 016204 (2002)
11. A. Shabunin, F. Baras, A. Provata, Phys. Rev. E **66**, 036219 (2002)
12. R.M. Ziff, E. Gulari, Y. Barshad, Phys. Rev. Lett. **56**, 2553, (1986)
13. X.G. Wu, R. Kapral, Physica A **188**, 284 (1992)
14. D.J. Liu, J.W. Evans, Phys. Rev. Lett. **84**, 955 (2000)
15. V.P. Zhdanov, Surf. Sci. Rep. **45**, 231 (2002)
16. A. Provata, G.A. Tsekouras, F.K. Diakonos, D.J. Frantzeskakis, F. Baras, A.V. Shabunin, V. Astakhov, Fluct. Noise Lett. **3**, L241 (2003)
17. H. Takayasy, *Fractals in the Physical Sciences*, (Manchester University Press, Manchester, 1990)
18. J. Feder, *Fractals* (Plenum Press, New York, 1988), and references therein
19. F. Esch, S. Günther, E. Schütz, A. Schaak, I.G. Kevrekidis, M. Marsi, M. Kiskinova, R. Imbihl, Surface Science **443**, 245 (1999)